Uncertainty Analysis of Near-Field Thermal Energy Transfer within Nanoparticle Packing

Anil Yuksel
Department of Mechanical Engineering
The University of Texas at Austin
Austin, TX 78712, USA

Edward T. Yu

Department of Electrical and Computer Engineering

The University of Texas at Austin

Austin. TX 78712. USA

Michael Cullinan

Department of Mechanical Engineering
The University of Texas at Austin

Austin, TX 78712, USA

Jayathi Murthy
Henry Samueli School of Engineering and Applied Science
University of California, Los Angeles
Los Angeles, CA 90095, USA

ABSTRACT

Laser heating of nanoparticles leads to significant near-field thermal effects between the nanoparticles. Due to the interaction between the laser and nanoparticle packings, some laser energy is scattered or absorbed, resulting in attenuation of the laser energy. The absorbed energy within the nanoparticles affects the near-field thermal energy transport. We have analyzed these effects by combining experimental determination of nanoparticle ink morphology with computational electromagnetic simulations. Scanning electron micrographs (SEM) of a representative copper nanoparticle ink show that the nanoparticles are distributed log-normally in size with 116 nm mean radius and 48 nm standard deviation. Hence, four instances of log-normally distributed copper nanoparticle packings which have 116 nm mean radius with 48 nm standard deviations are created by using a Discrete Element Model (DEM) in which a specified number of particles is generated, specifying a position and radius. Each nanoparticle is randomly generated with an initial velocity and a boundary under gravitational forces, which create the nanoparticle packing. Maxwell's equations in the frequency domain are simulated for these nanoparticle packings to understand the uncertainty analysis of near-field thermal energy within the nanoparticles by calculating the absorption, scattering and extinction coefficients. We show that nanoparticle distribution under gravitational forces doesn't significantly affect the absorption cross-section for both TE and TM polarization. Moreover, numerical and experimental results agree well between 400 nm to 800 nm wavelength of laser irradiation for generated different four particle distributions.

KEY WORDS: Near-field Thermal Energy, Polydisperse Nanoparticle Packing, Uncertainty Analysis

INTRODUCTION

Development of three-dimensional (3D) electronic packages has been one of the growing trends recently [1]. Due to providing multiple functionalities of these electronic packages, connectivity of these components will become crucial [2, 3]. However, such interconnects at microscale are not possible to be fabricated with traditional methods such as lithography due to the diffraction limit of the light [4]. There has been many efforts on using near-field optics to overcome the diffraction limit of the light, which makes vital to understand the near-field thermal energy transfer between the micro-nano structures [5, 6]. One of the recent growing progresses to overcome the diffraction limit of the light to fabricate sub-micron level interconnects is developing the microscale selective laser sintering (µ-SLS), where the high power laser energy is used as a heat source onto metal nanoparticle packings to create conductive structures [7]. When the high power laser interacts with the metal nanoparticles, localized surface plasmons could be exhibited which results very intense and non-local electromagnetic energy generation that drives the thermal energy transport [8]. Metal nanoparticles also show unique thermo-optical properties compared to their bulk material. Type, size, interparticle spacing between the nanoparticles and the medium properties affect the collective free electron oscillations within the nanoparticle packing [9], which characterizes the thermo-optical properties of the nanoparticle packings [10, 11]. Hence, the generation of nanoparticle packings is very important to understand the thermo-optical properties of the nanoparticle clusters under the high power laser source.

Discrete element method (DEM) is commonly used to generate the particle packing properties. In this method, each

particle is defined as a sphere with corresponding radius and position under the defined driving forces between the particles [12]. It has been observed from experiments that the copper nanoparticle ink has log-normally distributed with 116 nm mean radius in size and 48 nm standard deviation. Moreover, van der Waals forces between the nanoparticles are observed more dominant at much smaller in size and within dry nanoparticle packings [13]. Thus, we observed that nanoparticles under the gravitational force revealed a very similar nanoparticle distribution when compared with the SEM figures.

As the light confinement between the metal nanoparticle and the dielectric substrate is affected by the particle location, the plasmonic properties of the nanoparticle packings changes. Also, performing many trial- and-error experimental efforts result in huge time consumption along with high error. Thus, there is a need to perform uncertainty analysis to understand how iteratively and randomly generated nanoparticle packing affect the thermo-optical properties, which characterizes the near-field thermal energy transport. In this paper, generated four different nanoparticle packings - $(1\mu m \times 1\mu m)$ with ~ 400 nm thick- on a glass substrate and the same nanoparticle size distribution under gravitational force is investigated to understand the sensitivity of the thermo-optical properties for four randomly generated nanoparticle packings which gives insight into the near-field thermal transport.

The results will be used to predict the nanoparticle packing's temperature predictions on a glass substrate and provide insights into interconnect fabrication which utilize the photonic sintering.

EXPERIMENTAL MEASUREMENT

The absorptivity of the nanoparticle packings is obtained experimentally by a spectroscopy measurement as illustrated schematically in Fig. 1. A Cary 5000 UV-Vis-NIR (Agilent Technologies) is used to measure the transmittance and reflectance of ~400 nm thick Cu nanoparticle packing that is log-normal distributed and has 116 nm mean radius with 48 nm standard deviation and placed on a glass substrate with a wavelength range between 400 nm to 1064 nm. Absorptivity is then calculated as a function of wavelength from energy conservation by A=1-R-T

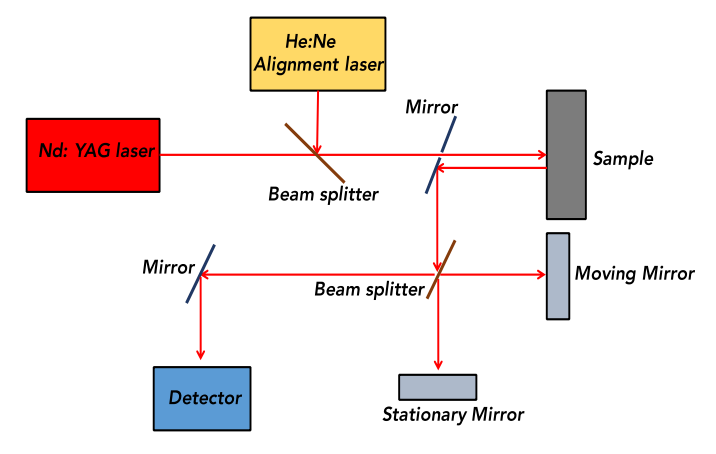


Fig. 1. Schematic of the spectroscopy measurement

COMPUTATIONAL ANALYSIS

An uncertainty analysis is performed in this section by analyzing the thermo-optical properties of four particle packings with the same particle size distributions that are generated by DEM. Fig. 2 illustrates the four randomly generated copper nanoparticle packings with 116 nm mean radius and 48 nm standard deviation. In these simulations, the gravitational force is the dominant interaction force on the particles that shapes the steady state particle configuration on a glass substrate, since the experimental measurements were taken on nanoparticle inks where van der Waals forces are insignificant.

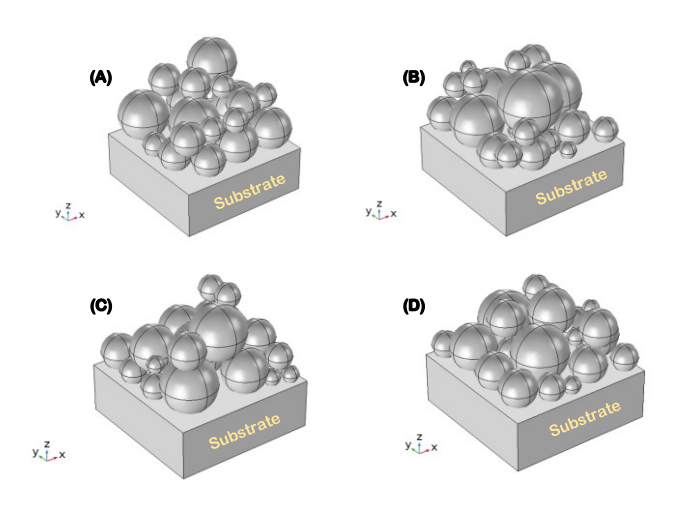


Fig. 2. Four different Copper nanoparticle packings generated by DEM that are lognormally distributed, 116 nm mean radius and 48 nm standard deviation, ~400 nm thick and placed on a 350 nm x 1000 nm x 1000 nm substrate

By applying TE and TM polarized, 532 nm laser illumination on particle packings, the absorption cross-section is analyzed and compared with the absorptivity value from spectroscopy measurements. Maxwell's equations are solved with respect to the scattered electric field by applying the Finite Difference Frequency Domain method, and the time-average Poynting vector for the time-harmonic field is calculated to obtain the energy flux. The total absorption efficiency is found by the integration of energy loss over the volume of all particles, and the scattering efficiency is calculated by surface integration of the scattered Poynting vector over an imaginary sphere covering all particles.

RESULTS

Fig. 3 shows that the simulated absorption cross-section decreases with increasing wavelength for TE and TM polarized light illumination when the wavelength of the light is greater than 532 nm. The absorption cross-section and absorptivity both have their highest values within 400 nm and 532 nm range. The average absorption cross-section for the four particle packings is found to be around 9.7*10⁻¹³ m² for the 400 nm and 532 nm TE and TM polarized light illuminations illustrated in Fig. 3. It is also observed that TE and TM polarized light has almost same absorption cross-section values indicating that the amount of light absorbed by

the nanoparticle packings is not highly dependent on the polarization of the light within these wavelength. However, the measured absorption cross-section values for TE and TM polarized light start to diverge at longer wavelengths. In fact, the effect of TM polarized light becomes larger than TE polarized light at 1064 nm though these results are still within the uncertainty of the simulations. However, this implies that there might be a higher wavelength than was measured where the effect due to the polarization might become important.

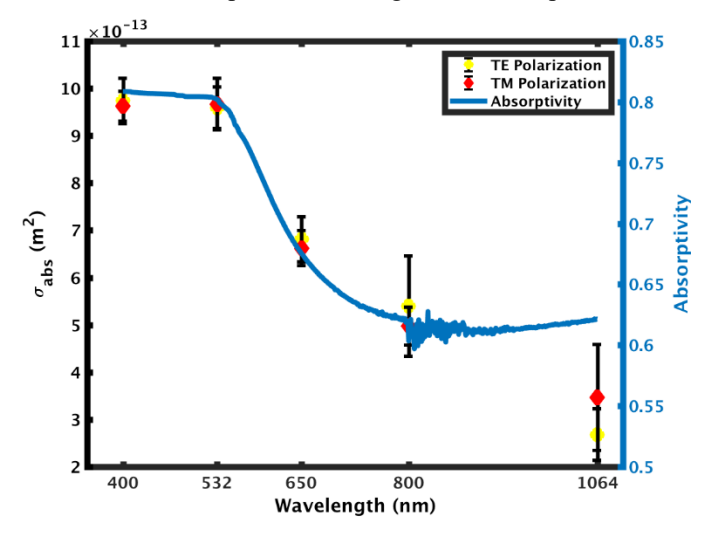


Fig. 3. Absorption cross-section (σ_{abs} (m²)), absorptivity vs. wavelength (nm) under TE and TM polarized laser illumination

Overall, the trends in the experimental absorptivity measurements match well with the calculated absorption cross section for the four nanoparticle packings simulated. Both the experiments and the simulations show relatively flat trends up to wavelengths of 532 nm followed by a decrease in absorption up to 800 nm. However, at 800 nm the measured absorptivity values level off at around 0.62 while the simulated absorption cross sections continue to decrease. This discrepancy could be due to the few nanometer PVP coatings on the nanoparticles that help keep them from agglomerating and oxidizing in the nanoparticle inks. The optical effects of this coating may get more important at higher wavelengths due to the permittivity properties of the coating material. In addition, some nanoparticles look like irregular shapes due to very strong clustering, and this type of nanostructure could influence the absorption spectrum. Indeed, this could result in scattering by particles such that multiple scattering and nondirectional scattering could become important at longer wavelengths for copper nanoparticles on a glass substrate. Also, the light source at 800 nm is switched to a near-IR light and the calibration of this light source might not be adjusted well so the data acquisition after 800 nm might not reflect the real trend.

The differences between the experimental and simulated results at longer wavelengths could be because the copper nanoparticle's skin depth decreases for wavelength higher than 532 nm so the closely packed nanoparticle's thermo-optical calculation from the finite element method

(FEM) could lead to higher error at longer wavelengths. The skin depth of a nanoparticle is calculated as follows:

$$\delta = \frac{1}{\text{Re}\sqrt{-k_0^2 \varepsilon_r}} \tag{1}$$

where k_0 is the free space wavenumber, and ε_r represents the complex relative permittivity function (Johnson and Christy (1972)).

Fig. 4 and Fig. 5 shows the relative permittivity and skin depth dependence on wavelength, respectively. The electron mean free path in copper is a constant at around 35.97 nm so as the wavelength of the light increases the difference between the electron mean free path and the skin depth also increases. For example, at around 532 nm the skin depth is almost equal to the mean free path but at 1064 nm the skin depth is only about two thirds of the mean free path. This could make the magnetic and electric field calculation in the simulation less accurate because of the extra collisions between the electrons at the surface of the particle, which quantum effects could start to become important when the skin depth is significantly less than the electron mean free path. In fact, the surface in the metal particle and the electron interactions in the conduction band become substantial. That results in extra collisions and this increases the damping which is also caused by the scattering of the electrons, impurities or lattice effects.

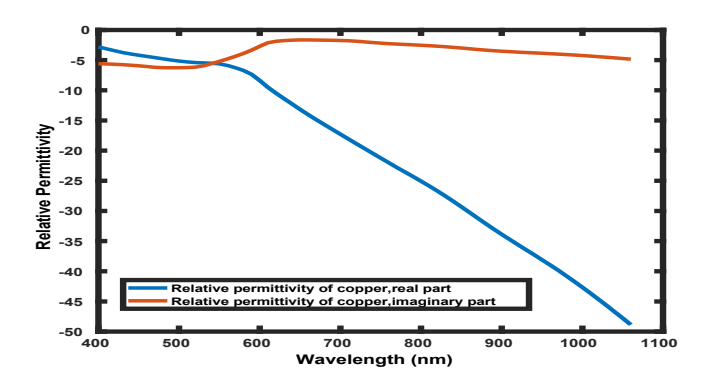


Fig. 4. Relative Permittivity vs. wavelength for copper nanoparticle

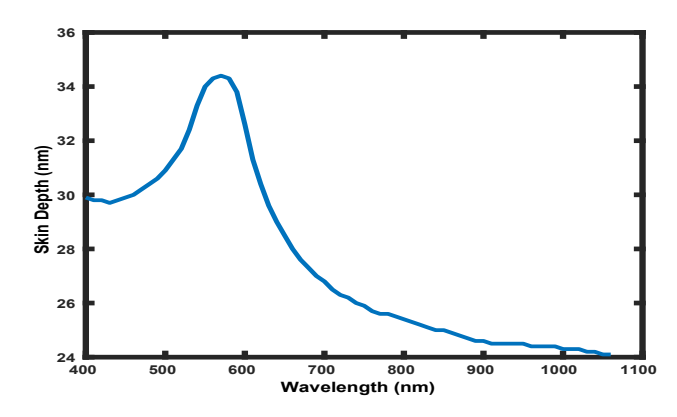


Fig. 5. Skin Depth vs. wavelength for copper nanoparticle

Scattering and Extinction Analysis of Nanoparticle Packings

Fig. 6 illustrates the scattering cross-section vs. wavelength for TE and TM polarized laser illumination. Due to the near-field scattering from the surface plasmon polaritons that are generated at 532 nm for copper nanoparticles, the scattering cross-section has this highest average value of around $7.5*10^{-13}$ m² at 532 nm under both the TE and TM polarizations. The scattering cross-section reaches its lowest average value of around $5*10^{-13}$ m² at 1064 nm. Also, it is observed that TE polarized laser has a higher average scattering cross-section value for each wavelength than TM polarized which may imply that the particles are arranged mostly along the TE polarized but this result is not statistically significant.

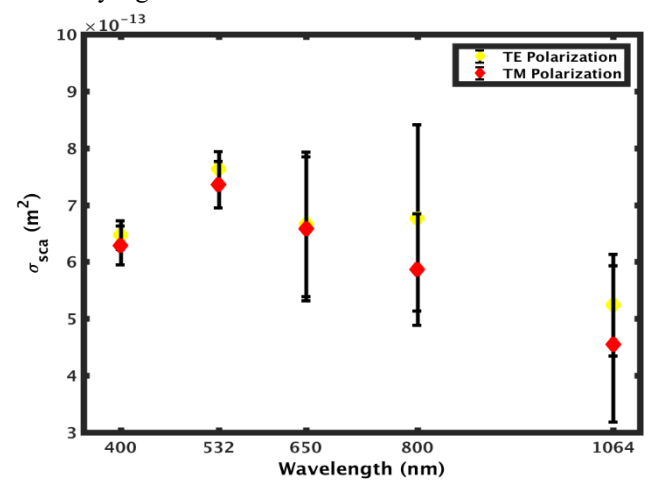


Fig. 6. Calculated scattering cross-section (σ_{sca} (m²)) vs. wavelength under TE and TM polarized laser illumination

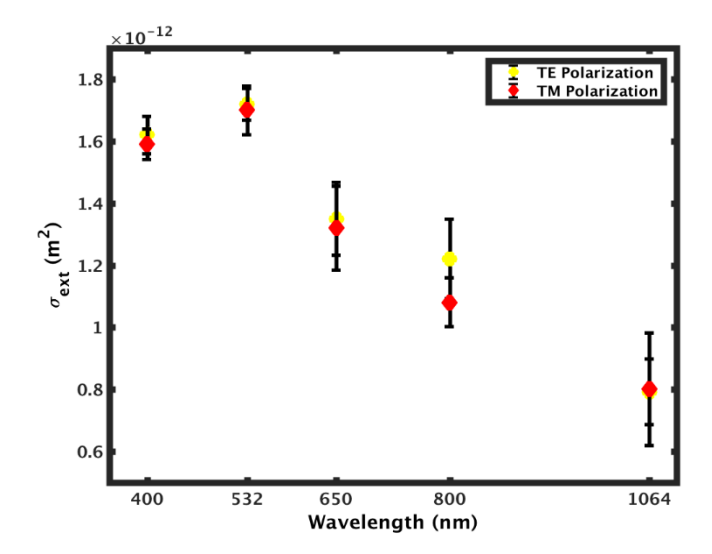


Fig. 7. Extinction cross-section (σ_{ext} (m²)) vs. wavelength analysis under TE and TM polarized laser illumination

Fig. 7 shows the extinction cross-section vs. wavelength under TE and TM polarized laser. It is observed that extinction cross-section reaches a maximum under the 532 nm laser illumination of around 1.7*10⁻¹² m². At

wavelengths higher than 532 nm, the extinction cross-section starts to decrease and becomes around $0.8*10^{-12}$ m² for 1064 nm light. Hence, the extinction cross-section can be reduced by around 50% by using wavelength 1064 nm as opposed to 532 nm. This implies that the light penetration into a nanoparticle packing is the narrowest at 532 nm wavelength laser between 400 nm and 1064 nm wavelength range. It is also seen that the polarization of the laser is not important on the extinction cross-section as the average TE and TM polarized light has almost the same value for each wavelength.

CONCLUSION

From our previous work, it is observed that nanoparticle size, spacing and the interparticle distance between the adjacent particles affect the thermo-optical properties and the plasmonic behavior of the nanoparticle packings. Also, as the nanoparticle packings generated randomly with DEM, uncertainty analysis is necessary to be able to understand how this randomness affects the simulated thermo-optical properties of the nanoparticle packing which we studied in this paper. Based on our analysis, exact location of the nanoparticle packings doesn't affect the absorption cross-section between 400 nm and 800 nm. Moreover, experimental and numerical result agree well within this wavelength range. As surface plasmon polaritons play a key role within the nanoparticles, 532 nm is observed the highest absorption which implies the enhanced near-field thermal transport over macroscopic length scales. However, the uncertainty range increases for scattering cross-section at wavelength above 532 nm. In overall, polarization and the exact particle location of nanoparticle packing on a glass substrate doesn't affect significantly the absorption and extinction cross-section. Thus, understanding of electromagnetic interaction between the nanoparticles is crucial to design and optimize the nanoparticle packings that can be tuned for desired application use.

ACKNOWLEDGEMENT

We would like to thank O. Georgina for providing the experimentally measured absorptivity data.

REFERENCES

- [1] Al-Sarawi, S. F., Abbott, D., & Franzon, P. D. (1998). A review of 3-D packaging technology. IEEE Transactions on Components, Packaging, and Manufacturing Technology: Part B, 21(1), 2-14.
- [2] Choudhury, D. (2010). 3D integration technologies for emerging microsystems. In Microwave Symposium Digest (MTT), 2010 IEEE MTT-S International (pp. 1-4). IEEE.
- [3] Emma, P. G., & Kursun, E. (2008). Is 3D chip technology the next growth engine for performance improvement?. IBM journal of research and development, 52(6), 541-552
- [4] D'Angelo, M., Chekhova, M. V., & Shih, Y. (2001). Two-photon diffraction and quantum lithography. Physical Review Letters, 87(1), 013602.
- [5] Betzig, E., & Trautman, J. K. (1992). Near-field optics: microscopy, spectroscopy, and surface modification beyond the diffraction limit. Science, 257(5067), 189-195

- [6] Boto, A. N., Kok, P., Abrams, D. S., Braunstein, S. L., Williams, C. P., & Dowling, J. P. (2000). Quantum interferometric optical lithography: exploiting entanglement to beat the diffraction limit. Physical Review Letters, 85(13), 2733
- [7] Roy, N., Yuksel, A. and Cullinan, M., 2016, "Design and Modeling of a Microscale Selective Laser Sintering System", ASME 2016 11th International Manufacturing Science and Engineering Conference (pp. V003T08A002- V003T08A002). American Society of Mechanical Engineers.
- [8] Roper, D. K., Ahn, W., & Hoepfner, M. (2007). Microscale heat transfer transduced by surface plasmon resonant gold nanoparticles. The Journal of Physical Chemistry C, 111(9), 3636-3641.
- [9] Daniel, M. C., & Astruc, D. (2004). Gold nanoparticles: assembly, supramolecular chemistry, quantum-size-related properties, and applications toward biology, catalysis, and nanotechnology. Chemical reviews, 104(1), 293-346.
- [10] Yuksel, A., Cullinan, M., & Murthy, J. (2017). Thermal Energy Transport Below the Diffraction Limit in Close-Packed Metal Nanoparticles. In ASME 2017 Heat Transfer Summer Conference (pp. V002T13A005-V002T13A005). American Society of Mechanical Engineers.
- [11] Yuksel, A., Edward, T. Y., Murthy, J., & Cullinan, M. (2017). Effect of Substrate and Nanoparticle Spacing on Plasmonic Enhancement in Three-Dimensional Nanoparticle Structures. Journal of Micro and Nano-Manufacturing, 5(4), 040903.
- [12] Kruggel-Emden, H., Simsek, E., Rickelt, S., Wirtz, S., & Scherer, V. (2007). Review and extension of normal force models for the discrete element method. Powder Technology, 171(3), 157-173.
- [13] Yuksel, A., & Cullinan, M. (2016). Modeling of nanoparticle agglomeration and powder bed formation in microscale selective laser sintering systems. Additive Manufacturing, 12, 204-215.